ROSAT PSPC Measurements of Periodic X-ray Variability in β Cephei Stars

David H. Cohen[1]
Bartol Research Institute, University of Delaware, Newark, Delaware, 19716. E-mail: cohen@bartol.udel.edu

John P. Finley
Department of Physics, Purdue University, West Lafayette, Indiana, 47907. E-mail: finley@purdys.purdue.edu

Joseph P. Cassinelli
Department of Astronomy, University of Wisconsin-Madison, Madison, Wisconsin, 53706. E-mail: cassinelli@madraf.astro.wisc.edu

ABSTRACT

We report the first detections of periodic X-ray variability in β Cephei variables. All four of our sample stars exhibit variability near or above the 3 σ level. The semi-amplitude is found to be 13% in ξ^1 CMa and 5% to 7% in the other three stars. The periods of the X-ray variability are in all cases consistent with the optical pulsation periods. These four detections nearly double the number of non-interacting-binary OB stars to show X-ray variability. Furthermore, these data have implications for the "wind-photosphere connection" in hot stars, as the X-rays arise in the wind and apparently respond to the periodic photospheric pulsations.

Subject headings: stars: atmospheres — stars: early-type — stars: individual (α Lup, β Cep, β Cru, ξ^1 CMa) — stars: oscillations — stars: variables: β Cephei — X-rays: stars

1. Introduction

The β Cephei stars are a class of early B stars that display regular low-amplitude photometric variability (generally $\Delta m_v \lesssim 0\overset{\mathrm{m}}{.}1$), radial-velocity variability (with amplitudes usually of order 10 km s^{-1}), and complex line-profile variability, all with periods between two and seven hours. The β Cephei instability strip is confined to a small region in the HR diagram extending from the zero-age main sequence up to luminosity class II-III (where core hydrogen burning is coming to an end), and from spectral type B0 to B2.5. These stars often show multiple, closely spaced periods due to a combination of radial pulsations and non-radial pulsations of low degree, ℓ. Both the wavelength-dependence of the photometric variability and the phase-lag between the radial velocity and photometric variability imply that the pulsation can be treated primarily as a change in the stellar effective temperature. An extensive review, emphasizing the photometric properties of β Cephei variables, can be found in Sterken & Jerzykiewicz (1993).

Although the variability of the prototype star, β Cephei itself, was discovered nearly one hundred years ago (Frost 1902), the cause of the pulsation has only been determined during the past decade. New opacities calculated by Iglesias & Rogers (1991) using the OPAL code developed at Livermore National

[1]also at Prism Computational Sciences, 16 N. Carroll St., Madison, Wisconsin, 53703. E-mail cohen@prism-cs.com

Laboratory show an increase in the iron opacity near $T = 200,000$ K with respect to previous calculations carried out at Los Alamos (Cox & Tabor 1976; Weiss, Keady, & Magee 1990). This increase is sufficient to drive the pulsational instability in β Cephei variables via the opacity-, or κ-mechanism (Moskalik & Dziembowski 1992; Kiriakidis, El Eid, & Glatzel 1992).

Until now, the X-ray properties of β Cephei variables have been found to be generally ordinary. That is, they are very similar to other hot (OB) stars, especially other early B stars. β Cephei stars have X-ray luminosities that roughly follow the empirical $L_X/L_{Bol} \approx 10^{-7}$ law (Agrawal et al. 1984) which holds for all O and very early B stars (Pallavicini et al. 1981; Cassinelli et al. 1994). They have soft *ROSAT PSPC* spectra, like other early B stars (Cohen, Cassinelli, MacFarlane 1997a), although there is some evidence from the *ROSAT All-Sky Survey* that the β Cepheis have even softer spectra than other hot stars (Meurs et al. 1992). Finally, very little significant X-ray variability has been detected in β Cephei variables (Agrawal et al. 1984; Drew, Denby, & Hoare 1994; Cohen et al. 1997a). This is in accord with the usual behavior of hot stars, which show remarkably time-steady X-ray emission properties (Berghöfer & Schmitt 1995). Most of the previous X-ray observations of β Cephei variables covered less than a single optical period, however, so the conclusion of no X-ray modulation in these stars is tentative.

It is generally accepted that the X-ray emission, which is ubiquitous in OB stars, arises in the fast stellar winds of these objects and is somehow related to the instability inherent to line-driven outflows (Lucy & Solomon 1970; Owocki, Castor, Rybicki 1988). It appears that self-excited instabilities cannot generate sufficient X-ray emission in most early-type stars (Cooper & Owocki 1994; Feldmeier 1995), but some type of perturbation near the stellar surface might be able to enhance the X-ray shock-emission when dense clumps collide far out in the winds of hot stars (Feldmeier, Puls, & Pauldrach 1997). However, this X-ray production mechanism has only been explored in the very dense winds of O supergiants. There is also some evidence, especially in young hot stars (Cohen, Cassinelli, & Waldron 1997b) and late-B stars (Berghöfer & Schmitt 1994a), that instability-generated wind shocks, no matter how efficient, are incapable of producing all of the observed X-rays, in which case processes involving magnetic fields or a combination of magnetic fields and weak radiation-driven winds are invoked. Finally, it should be pointed out that the best-studied O stars (Nordsieck, Cassinelli, & Anderson 1981; MacFarlane et al. 1993; Corcoran et al. 1993) and B stars (Cohen et al. 1996) show strong evidence that the X-ray emission arises *within* the stellar winds, regardless of the exact mechanism that produces it.

There has been a lot of attention focused recently on the "wind-photosphere connection" (*e.g.* Kaper et al. 1997), in which various observational means have been employed to determine how close to the stellar surface wind structure and variability begins, and to search for connections between photospheric and wind variability. This effort has been primarily focussed on UV absorption line profile variability, and specifically on the evolution of discrete absorption components from low wind velocities to high velocities (see *e.g.* Massa et al. 1995). Berghöfer et al. (1996) have detected correlated Hα variability and low-amplitude X-ray variability in ζ Pup (O4 If). The Hα emission arises in the dense base of the stellar wind, so these data indicate that disturbances can propagate from the base of the wind, just above the stellar photosphere, to many tens of stellar radii, where the X-rays we see are formed in this star. Any measurement of a relationship between *photospheric* variability and X-ray emission would extend the evidence of a direct wind-photosphere connection.

Aside from ζ Pup, only a handful of OB stars which are not in interacting binary systems have confirmed measurements of X-ray variability. The Be star λ Eri brightened by a factor of 6 during a *ROSAT PSPC* observation (Smith et al. 1993). This brightening was due entirely to photons with $h\nu \gtrsim 0.7$ keV, and the authors characterize the event as an X-ray flare, in an analogy to coronal events on the sun and solar-like stars. The O star ζ Ori was seen to increase in brightness by at least 30 percent over a period of several days in 1992, which was attributed to a single large shock propagating through the stellar wind (Berghöfer & Schmitt 1994b). Collura et al. (1989) detected variability in the *Einstein* IPC observations of the B supergiant δ Ori (on timescales of days) and in Cyg-OB2 8A (on timescales exceeding 10^4 s). The very strong X-ray source γ Cas (B0.5 Ve) shows X-ray variability anti-correlated with ultraviolet absorption line strength variability (Smith, Robinson, & Corbet 1998). Finally, Cohen et al. (1997a) found low-level variability in short *ROSAT* observations of the B stars β Cen (which is a β Cephei variable) and μ Cen (which is a Be star). In all of these cases (aside from ζ Pup and γ Cas), the variability gives no indication of being periodic, or being associated directly with photospheric activity. The only other detections of X-ray variability in hot stars involve interacting binaries and extreme types of stars, such as η Car (Corcoran et al. 1997). In general, OB stars show remarkable time constancy in their X-ray emission (especially considering the highly variable nature of the shocked stellar winds indicated by numerical simulations and UV and Hα observations).

In this paper we report on long *ROSAT PSPC* observations of four well-known β Cephei variable stars. These observations are significantly longer and more sensitive than those used for previous X-ray studies of β Cepheis. Our goals are to determine if these variable stars are truly as time-constant as the vast majority of hot stars, or if there might be X-ray variability associated with atmospheric pulsations. Specifically, we would like to know if the X-ray flux is modulated on the same period as the optical variability, and if so, whether the variability is primarily in the soft or hard X-ray band. The soft band is strongly affected by wind *absorption*, whereas the hard X-ray band reflects the intrinsic X-ray *emission* process (Owocki & Cohen 1999), and we would like to know whether the variability is representative of a change in the X-ray production mechanism, or simply in the density of the ambient wind flow. If X-rays are associated with the optical variability seen in β Cepheis, it would be one of the most direct observations to date that links photospheric activity with wind activity in a hot star.

In §2 we describe the sample of four β Cephei stars. In §3 we describe the *ROSAT* observations. In §4 we analyze the data. A discussion is presented in §5, and conclusions are summarized in §6.

2. The Stars

The four stars included here are all well-studied, bright β Cephei variables with extensive databases of optical variability measurements, and in most cases UV data as well. The basic properties of the stars are listed in Table 1. In the rest of this section we elaborate on the pulsation properties of the sample stars, as well as some other relevant properties of specific stars.

In general, β Cepheis have several closely spaced periods, and while α Lup has two known photometric and radial velocity periods, until recently the other three stars in this study each had only a single period determined from photometric and spectroscopic observations (Heynderickx 1992). However, recent studies have found additional periods due to non-radial pulsations for β Cep and β Cru (Aerts et al. 1994; Telting, Aerts, & Mathias 1997; Aerts et al. 1998). Additionally, β Cep shows two further periods which are probably due to rotational splitting (Telting et al. 1997). For β Cru the main period is due to non-radial pulsations of order $\ell = 1$, but for the other three stars the primary periods are attributed to radial pulsations. The variability data are summarized in Table 2. We will, however, confine the variability analysis in this paper to the well-established periodicities listed in Heynderickx (1992). These are the primary periods for β Cep, ξ^1 CMa, and β Cru and the primary and secondary periods for α Lup.

Table 1. Sample Stars

Star	Spectral Type	m_v	Distance[a] (pc)	L_B[b] (ergs s^{-1})	$\dot{M}$[c] ($M_\odot$ yr $^{-1}$)	v_∞[c] (km s^{-1})
β Cep[d]	B1 III	3.19	182 ± 16	1.5×10^{38}	2.8×10^{-8}	1650
ξ^1 CMa[e]	B1 III	4.33	629 ± 277	1.5×10^{38}	2.8×10^{-8}	1650
β Cru[e]	B0.5 III	1.25	108 ± 7	2.4×10^{38}	5.6×10^{-8}	2000
α Lup[e]	B1.5 III	2.30	168 ± 21	1.0×10^{38}	1.2×10^{-8}	1400

[a]From the Hipparcos catalog (ESA 1997).

[b]Estimated values based on the spectral type and luminosity class using the calibration of Straizys & Kuriliene 1981.

[c]Theoretical values based on the spectral type and luminosity class using the α, k, δ tabulation of Abbott 1982.

[d]Spectral type and apparent magnitude from Lesh 1968.

[e]Spectral type and apparent magnitude from Hiltner, Garrison, & Schild 1969.

Table 2. Pulsation Periods

Star	Period (hr)	Comments
β Cep	4.571625	photometric;[a] radial mode[b]
	4.4610	non-radial[b] $\ell = 1$ or 2
	4.8780	non-radial[b] $\ell = 1$ or 2
ξ^1 CMa	5.02809	photometric;[a] radial mode[c]
β Cru	4.58843	photometric;[a] non- radial[d]
	4.027747	non-radial[d] with $\ell = 3$
	4.38583	non-radial[d] with $\ell = 4$
α Lup	6.23632	photometric;[a] radial mode[c]
	5.683	photometric;[a] non-radial[c] $\ell = 1$

[a]Heynderickx 1992.

[b]Telting, Aerts, & Mathias 1997.

[c]Heynderickx, Waelkens, & Smeyers 1994.

[d]Aerts et al. 1998.

Beeckmans & Burger (1977) used satellite UV data to determine that the peak to peak photometric variability near 2100 Å is $0^{\rm m}_{.}07$ for β Cep and $0^{\rm m}_{.}08$ for ξ^1 CMa. UV variability data at several wavelengths was used to determine a mean effective temperature change of 1340 ± 360 K for β Cephei and 1400 ± 430 K for ξ^1 CMa.

Regarding binarity, all four of the stars have binary companions but there is no indication of any binary interaction in any of the four stars, with the exception of the possibility of tidal forcing of some of the pulsation modes in β Cru (Aerts et al. 1998). Two of the stars have visual companions, while the other two have spectroscopic companions. Though we cannot rule out a contribution to the overall X-ray emission from the binary companions, the level of contamination should be small based on the relatively large fluxes of early-B stars and the spectral types of the companions. This is confirmed by the fact that the spectral properties of all the program stars are relatively soft, like other B stars, and unlike nearly every later-type star.

The prototype β Cep is actually quite unusual in that it is both a Be star (Sahade & Struve 1956) and a magnetic Bp star with a varying field strength (Henrichs 1993). This field has recently been measured to be $B = 100 \pm 40$ G and is varying in polarity due to stellar rotation (Henrichs et al. 1999). The presence of a magnetic field might affect X-ray production via dynamo activity or through magnetic confinement of a radiation-driven wind. The *ROSAT* data was taken at the beginning of the most recent period of Be disk growth, with $H\alpha$ increasing in emission strength for at least one year before the observations were made (Henrichs et al. 1999).

3. The *ROSAT PSPC* Observations

All of the data were taken with the *ROSAT* position-sensitive proportional counter (*PSPC*) as part of NASA's guest observer program. The telescope, which has an energy-dependent effective area of several hundred cm^2 over a range of 0.1 keV to 2.4 keV, is described in Trümper (1983). The *PSPC* (Pfeffermann et al. 1986) provides a spectral resolution of $\lambda/\Delta\lambda \approx 2.3(h\nu/0.93\,{\rm keV})^{1/2}$, and in combination with the telescope's grazing incidence mirror, has a spatial resolution with a FWHM of approximately $25''$. The background noise levels are very low and well characterized compared to earlier X-ray telescopes (Briel et al. 1996).

These observations cover at least several days each, but due to gaps in the data the effective exposure times are comparable only to the optical pulsation periods ($t \approx 5$ hr). The details of the observations are shown in Table 3. It should be noted that β Cru has an exceptionally high *ROSAT* count rate for a near-main-sequence B star.

We extracted source counts from the raw data using a circular region centered on the location of each target, and large enough to include any "ghost images" due to soft photons ($h\nu \lesssim 0.15$ keV), which cannot be effectively localized in the detector (Nousek & Lesser 1993). Because all of the sources are bright and the background flux levels are low, we did not perform a background subtraction. To test the resulting accuracy, we examined background diffuse fluxes and other point sources in each field for variability and found none. We describe the time-variability analysis in the next section.

In order to determine the general, *time-averaged* spectral properties of the four program stars, we fit the *PSPC* spectra with standard plasma emission models. We prepared spectra by extracting the source counts in the same way as described above for the light curves. Here, however, we also extracted background spectra for each observation using a source-free region from a location near each β Cephei star (whenever possible from an annulus around the source extraction region). Both were binned in energy such that each bin had at least ten counts. We subtracted the background spectrum from the source-plus-background spectrum, and fit differential emission measure models (assuming a continuous temperature distribution) that account for both wind attenuation and interstellar attenuation, as described in Cohen et al. (1997a). All four stars have normal X-ray spectral energy distributions for late-O and early-B stars. That is, the best-fit differential emission measure models are weighted heavily toward low temperatures ($\frac{dEM}{dT} \sim T^{-2}$), and a modest amount of wind attenuation of the generated X-rays is seen. The X-ray luminosities and $L_{\rm X}/L_{\rm Bol}$ values are listed in Table 4. The best-fit models along with the *PSPC* data are shown in Figure 1.

4. Data Analysis

To assess time variability, we first tested the null hypothesis of a constant source for each star. To do this, we binned each data set according to the known optical periods. The time-tagged detector events were placed in one of 20 equally spaced phase bins. For each bin, a correction factor was applied, based on the fraction of the time that the detector was observing the source. Error bars were assigned to each bin's count rate according to photon-counting poisson statistics. Note that in the case of α Lup, the two different periods produce different light curves.

We then calculated the χ^2 statistic for each light curve and a constant source model having the mean observed *ROSAT PSPC* count rate. These χ^2 values, along with the degrees of freedom for each data set, are listed in Table 5. Also shown in this table are the probabilities that a χ^2 lower than the actual value would be obtained simply from statistical variations with the assumed constant source model. These values can be interpreted as the significance level of variability for each data set. A high P-value therefore indicates that the source is variable. In Table 5 we also show the χ^2 and P values for an unrelated source or background region in each field. This was done to demonstrate that any source variability detected is not due to instrumental effects.

For β Cru and ξ^1 CMa, the null hypothesis can be rejected at better than the 99% level, so the evidence for variability is correspondingly strong. For the other two stars, the null hypothesis can be rejected at somewhat above the 95% level, making determinations about variability slightly less certain. To explore the nature of the variability, we formed light curves and calculated the χ^2 statistic in the same way for the

Table 3. Observation Log

Star	Observation Dates (U.T.)	Exposure Time (s)	Count Rate (counts s^{-1})
β Cep	1992 August 26 (10:11) to 1992 August 27 (10:57)	15,355	$0.233 \pm .004$
ξ^1 CMa	1992 April 3 (7:34) to 1992 April 5 (8:19)	1,991	$0.115 \pm .007$
	1993 April 1 (11:24) to 1993 April 4 (6:54)	15,440	$0.137 \pm .003$
β Cru	1993 July 12 (10:48) to 1993 August 27 (1:43)	12,401	$1.453 \pm .011$
α Lup	1993 August 22 (3:25) to 1993 August 26 (13:04)	17,279	$0.105 \pm .002$

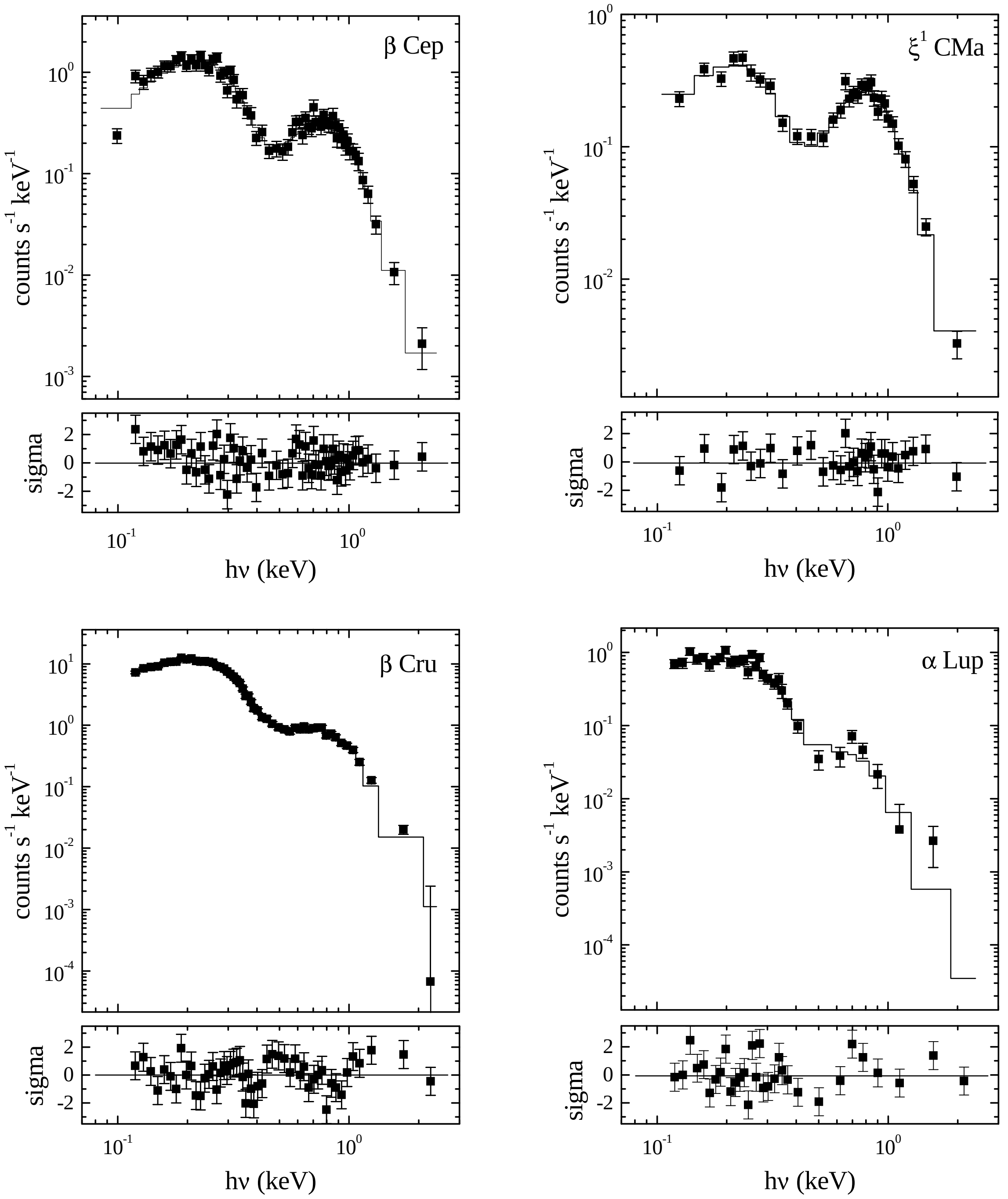

Fig. 1.— Spectral energy distributions (points with error bars) for each of the four program stars along with the best-fit models (lines).

Table 4. X-ray Luminosities

Star	$L_{\rm X}^{\rm o}$ [a] (ergs s^{-1})	$L_{\rm X}^{\rm o}/L_{\rm Bol}$
β Cep	2.7×10^{31}	1.8×10^{-7}
ξ^1 CMa	3.9×10^{31}	2.6×10^{-7}
β Cru	3.9×10^{31}	1.6×10^{-7}
α Lup	8.3×10^{30}	8.3×10^{-8}

[a]The X-ray luminosity *emergent* from the stellar winds is denoted by $L_{\rm X}^{\rm o}$. For these stars this quantity is somewhat (about a factor of two) less than the total X-ray luminosity *produced* in the wind.

Table 5. Testing the Null Hypothesis

Star	Period (hr)	χ^2	P (%)	d.o.f.
β Cep	4.571625	30.3	97.6	17
comparison source	4.571625	17.3	57	17
ξ^1 CMa	5.02809	39.7	99.9	17
comparison source	5.02809	10.7	13	17
β Cru	4.58843	52.0	99.9997	14
comparison source	4.58843	12.5	44	14
α Lup	6.23632	20.8	92.3	13
comparison source	6.23632	12.4	51	13
α Lup	5.683	27.6	96.5	16
comparison source	5.683	14.6	45	16

hard (0.5 keV $\lesssim h\nu \lesssim$ 2.4 keV) and soft (0.1 keV $\lesssim h\nu \lesssim$ 0.4 keV) data. These results are listed in Table 6. In the case of ξ^1 CMa, the variability is completely attributable to the soft band. However, for β Cru, while the soft band shows some variability, the hard band dominates the overall variability. Relatively significant variability is indicated in the soft band for α Lup. The indications of variability in β Cep are less significant for either of the bands individually than for the entire bandpass as a whole, although there is more indication of significant variability in the soft band. This could be due simply to the lower signal-to-noise of the energy-binned data.

To further explore the X-ray variability of these four stars, we used the optical periods to fit sinusoidal models to the binned light curves. Although the optical periods were used for this model fitting, the amplitudes and phases were fit as free parameters. In Figure 2 we show the binned data with error bars along with the mean count rate and the best-fit sinusoidal model. These parameters are listed in Table 7. The fits are relatively good, but due to a handful of outlier points, the formal χ^2_ν values are still somewhat greater than unity. We also fit sinusoidal models to the soft and hard bands separately, and these results are summarized in Table 8.

The sinusoidal fits demonstrate the significance of variability by the levels of the fitted amplitudes and their uncertainties. The fit to the total light curve for β Cru, shown in Figure 2, has a relative (half-) amplitude of $4.8 \pm 1.4\%$, implying a 3.5 σ significance level of variability. The largest variability is seen in ξ^1 CMa with an amplitude of $12.9 \pm 3.6\%$, which also implies a 3.5 σ significance level. The β Cep and α Lup amplitudes have significance levels slightly less than 3 σ (with the second period for α Lup showing higher significance than the first). Note that all these results are consistent with the results of the null-hypothesis testing. The amplitudes of the sinusoidal fits to both the hard- and soft-band light curves show significant variability in β Cru and ξ^1 CMa, while the individual bands show variability with significance between 2 σ and 3 σ for the other two stars.

Finally, we examined the correlations between the hardness of the *PSPC* spectra and the total count rate. We have shown that in some cases the variability is dominated by the soft band, and in other cases by the hard band. It is of interest to know whether the overall modulation is due to an increase or a decrease in flux in one of the bands. We calculated correlation coefficients for the hardness ratio ($(hard - soft)/total$) and the total count rate for each data set. In no case was the result significant at better than the 90% level. This lack of significant correlation could very well be due to the relatively poor signal-to-noise of the hardness ratios.

Table 6. Testing the Null Hypothesis for Hard and Soft Bands

Star	Period (hr)	χ^2_{soft}	P_{soft} (%)	χ^2_{hard}	P_{hard} (%)	d.o.f.
β Cep	4.571625	21.9	81.0	24.9	90.2	17
ξ^1 CMa	5.02809	35.4	99.4	15.0	40	17
β Cru	4.58843	31.8	99.6	81.2	> 99.9999	14
α Lup	6.23632	25.9	98.3	28.0	99.1	13
α Lup	5.683	33.2	99.3	16.6	59	16

Table 7. Sinusoidal Model Fits

Star	Period (hr)	Count Rate (counts s^{-1})	Amplitude (counts s^{-1})	Amplitude (fraction of mean)
β Cep	4.571625	0.223	$0.015 \pm .006$	0.067 ± 0.027
ξ^1 CMa	5.02809	0.134	$0.018 \pm .005$	0.129 ± 0.036
β Cru	4.58843	1.453	$0.070 \pm .020$	0.048 ± 0.014
α Lup	6.23632	0.105	$0.003 \pm .003$	0.029 ± 0.029
α Lup	5.683	0.105	$0.007 \pm .004$	0.067 ± 0.038

Table 8. Sinusoidal Model Fits to Hard and Soft Bands

		Soft		Hard	
Star	Period (hr)	Count Rate (counts s^{-1})	Amplitude (counts s^{-1})	Count Rate (counts s^{-1})	Amplitude (counts s^{-1})
β Cep	4.571625	$0.137 \pm .003$	$0.010 \pm .004$	$0.085 \pm .002$	$0.007 \pm .003$
ξ^1 CMa	5.02809	$0.055 \pm .002$	$0.008 \pm .002$	$0.079 \pm .002$	$0.009 \pm .003$
β Cru	4.58843	$1.14 \pm .01$	$0.042 \pm .018$	$0.251 \pm .008$	$0.039 \pm .012$
α Lup	6.23632	$0.087 \pm .003$	$0.007 \pm .003$	$0.015 \pm .001$	$0.005 \pm .002$
α Lup	5.683	$0.090 \pm .003$	$0.007 \pm .003$	$0.015 \pm .001$	$0.003 \pm .001$

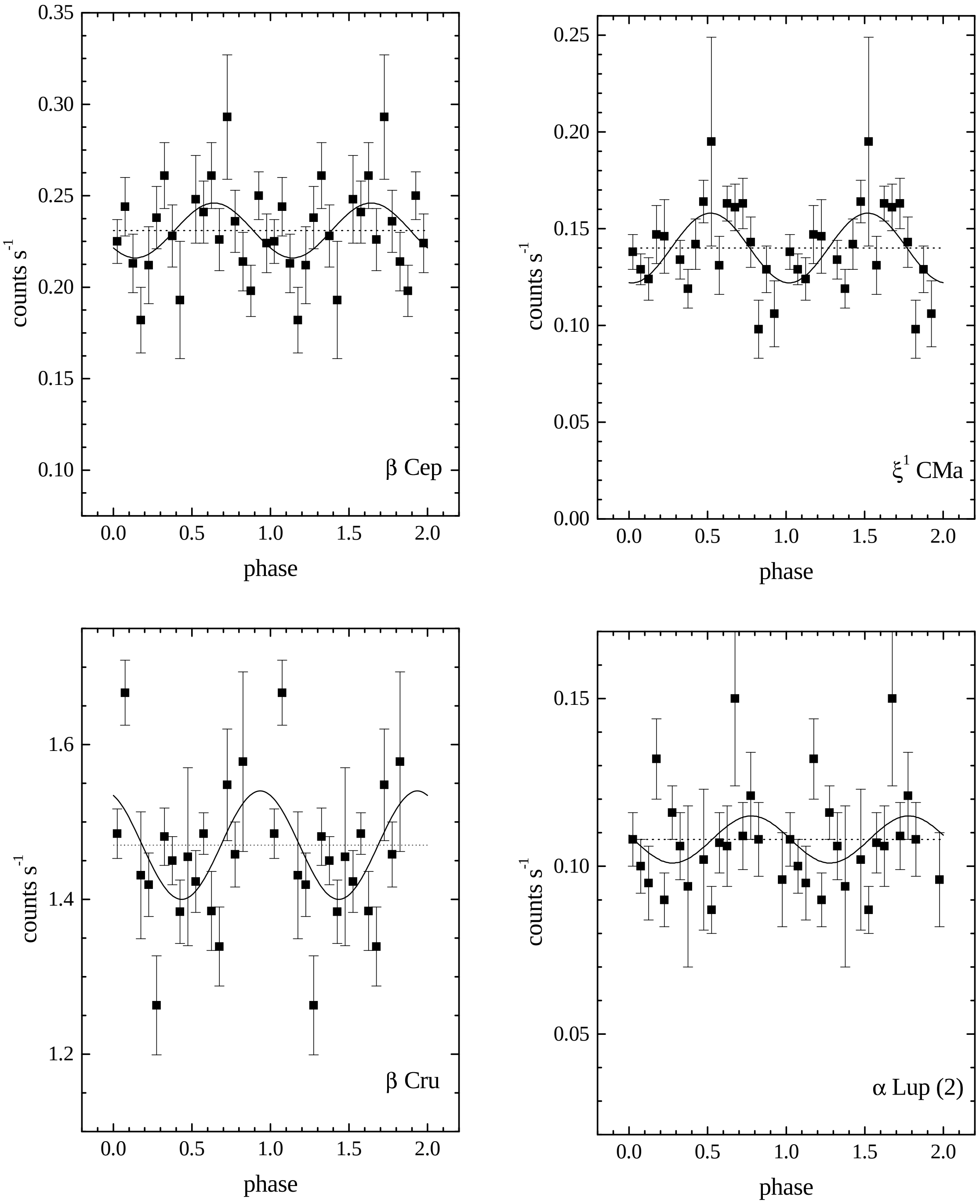

Fig. 2.— Phased and binned *ROSAT* light curve for each of the four sample stars ((a) β Cru, (b) ξ^1 CMa, (c) β Cep, (d) α Lup (secondary period)), shown with mean count rate and best-fit sinusoidal model.

5. Discussion

The most general assumption about hot star X-rays that is consistent with observations is that the X-ray emitting gas is contained in so many individual small structures that it can be approximated by a continuous spatial distribution. This distribution begins at some lower radius (perhaps $r \approx 1.5$ to 2 R_*), and is characterized by a filling factor (as a fraction of the total mass in the wind or, alternately, of the total emission measure) that describes the efficiency with which a given wind produces X-rays. This picture is consistent with numerical simulations of the line-force instability (Cooper & Owocki 1994; Feldmeier 1995), but is more generally applicable to many different wind-shock models. It should be noted that in this picture of embedded wind shocks that the ambient unshocked wind may be optically thick to X-rays, especially very soft X-rays. Owocki & Cohen (1999) have recently shown that for an X-ray filling factor that is independent of radius, at energies at which a wind is completely optically thick the X-ray emission scales with the density, whereas for a completely optically thin wind it scales with the square of the density.

If the X-ray production efficiency is constant for a β Cephei wind as the star undergoes a pulsation cycle, then the overall level of X-ray emission might still vary due to the change in the wind density (via the mass-loss rate) caused by the change in the star's luminosity (and effective temperature). To estimate the change in the wind density as a function of pulsation phase, we can examine the steady-state CAK (Castor, Abbott, & Klein 1975) wind solutions for the two extreme phases. As we discussed in §2, UV data suggests that $T_{\rm eff}$ changes by 1400 K in ξ^1 CMa from its low to high pulsation state. We find from Abbott's (1982) tabulation of CAK parameters, that the mass-loss rate changes by a factor of 3 for a change in effective temperature of 1400 K (which corresponds to a $\pm 20\%$ change in luminosity for a $T_{\rm eff} \approx 26,500$ K star like ξ^1 CMa), from $\dot{M} \approx 1.4 \times 10^{-8}$ $M_\odot$ yr $^{-1}$ to $\dot{M} \approx 4 \times 10^{-8}$ $M_\odot$ yr $^{-1}$. The terminal velocity changes only by 150 km s^{-1} between these two states, according to these CAK parameters (but see the discussion later in this section about the bistability jump).

Can this factor of three change in the wind density account for the roughly 5% to 15% change in the X-rays even if the X-ray production efficiency remains constant? To answer this question, we need to examine how a ~ 5 hour cyclical variation of the mass-loss rate affects the *global* wind density structure. Even at the wind terminal speed, a density enhancement (or rarefaction) travels only about 5 R_* during one pulsation cycle. So, as one looks into such a hot star wind, a series of density waves are encountered and to obtain the total emergent X-ray luminosity this distribution must be integrated down to some reasonable lower limit. This is either the radius at which X-ray production begins or the radius at which the wind becomes optically thick. Because at any one time there is an averaging over both lower- and higher-density regions it is expected that the total mass or emission measure in the wind will vary by substantially less than does the instantaneous mass-loss rate.

We have assessed the expected level of X-ray variation in a wind from a pulsating hot star by numerically calculating a CAK wind model in which we varied the luminosity sinusoidally with a 20% (half-) amplitude and a 5 hour period. We then integrated the emission measure, $EM = \int n^2 dVol$, from some large radius down to a reasonable lower value of the radius, $R_{\rm min}$. It is the emission measure that is relevant because the X-rays arise from two-body collisional processes. The farther down in the wind (closer to the star) the emission measure integration is carried out, the more variability is seen. This is because the density (and especially the density squared) decreases very rapidly with radius, so the closer to the stellar surface the integration is carried out the more it is dominated by a thin layer near the star. And the smaller the region that dominates the emission measure integration, the more a single pulsation-induced density enhancement affects the total emission.

In Figure 3 we show the density squared at each point in the wind as a function of time through several pulsations. By looking at horizontal cuts through these data, one can see that two cycles of density enhancement are present in the first few stellar radii. We note that the contribution to the total emission measure of material with $r \gtrsim 10$ R$_*$ is negligible. The emission measure integral from this model gives roughly a 10% (half-amplitude) level of variability when the lower limit of integration is 2 R$_*$ (from the center of the star, 1 R$_*$ above the surface). This 10% variability is relatively constant as the limit of integration decreases to about $R_{\rm min}$ = 1.25 R$_*$. Although, if the lower radius of the emission measure integral is below this there is a strong increase in the level of variability seen in the emission measure. For example, if $R_{\rm min}$ = 1.1 R$_*$ then the half-amplitude of variability for the emission measure is 25%. These β Cephei variables are expected to have winds that are optically thick at all relevant energies at a depth of r = 1.1 R$_*$, however. Finally, bear in mind that these numbers represent variations in the X-ray emission due *only* to variations in a star's mass-loss rate caused by pulsation-driven photospheric variability and *not* due to changes in the X-ray production efficiency that might also be caused by the pulsations.

These calculations assume that attenuation of X-rays by the cold ambient wind does not vary (and indeed is negligible down to the lower limit of integration). At sufficiently low photon energies, however, the wind will be optically thick[1], and its optical thickness will increase with increasing mass-loss rate. The added attenuation during times when the mass column through the wind is larger will tend to decrease the level of X-ray variability by as much as 50%.

Thus, for the strongest X-ray variable in our sample, ξ^1 CMa, the simple mechanism of time-variable wind density and a constant X-ray production efficiency may not be quite enough to explain the observed variability. However, the observational uncertainty makes this conclusion far from secure. For the other three stars, which show a lower level of variability, the variation in the mass-loss rate, and thus the emission measure, may be a sufficient explanation even if the onset of X-ray production does not occur until $r \approx 2$ R$_*$. These data, therefore, are not inconsistent with the X-ray modulation arising from periodic changes in the wind density caused by the photospheric variability, although for ξ^1 CMa, the consistency is marginal and requires an onset of X-ray production at only a few tenths of a stellar radius.

We cannot, however, rule out the possibility that the photospheric pulsations cause changes in the X-ray production *efficiency* in the wind and not just in the total amount of material in the wind. It should be noted that when different sectors of a star's surface are characterized by different temperatures that wind streams having different properties will be driven from the star, and these wind streams may interact with each other leading to shocks that may produce X-rays (Mullan 1984; Cranmer & Owocki 1996). This could occur especially in β Cru, which is primarily a non-radial pulsator. We note that in the case of α Lup, the secondary period, which shows much more significance than the primary period in terms of X-ray variability, is also a non-radial mode. This could indicate that non-uniformities on the stellar surface may play an important role in the variable component of the X-ray emission in β Cephei stars. The magnetic field in β Cep may also play a role in the X-ray production in this star–either through magnetic confinement of the wind or by seeding instabilities which may lead to shock-produced X-rays. However, β Cephei is one of the less variable stars in our study, so there is no reason to insist that magnetic fields play an important role in the phenomenon of X-ray variability in β Cepheis.

It is also possible that the wind streams from the lower- and higher-density phases interact with each other in such a way as to enhance the X-ray emission. This would be more likely if the pulsational changes

[1]At $h\nu = 200$ eV, optical depth unity is reached at $r \approx 1.5$R$_*$ for a B1 III star (Owocki & Cohen 1999).

in the stellar properties caused the β Cephei stars to traverse the bistability jump (see Pauldrach & Puls 1990). This is not indicated by the tabulation we are using to generate wind models in this paper (Abbott 1982), but it is possible that a new calculation of the CAK parameters for B stars could show the β Cepheis straddling the bistability jump. Crossing the bistability jump during a pulsation cycle could cause the high mass-loss rate mode to have a significantly higher velocity than the low mass-loss rate mode. And the fast and slow wind streams could then interact causing a driven shock (as in MacFarlane & Cassinelli 1989). This mechanism is perhaps not likely to produce strong X-rays however, as the wind flow times are short compared to the pulsation (and X-ray variability) timescales.

It appears that deeper insight into the detailed changes in the X-ray production driven by stellar pulsations awaits the much higher resolution spectroscopy available with *AXAF*, *XMM*, and *ASTRO-E*. These telescopes, with spectral resolution $\lambda/\Delta\lambda > 100$ will allow for detailed measurements of variability in emission line ratios, continuum attenuation, absorption edge wavelengths and decrements, and perhaps even line widths. This will allow for the determination of how pulsations affect the temperature distribution and density in the emitting plasma, how they affect the ambient unshocked wind, and how the velocity-distribution of X-ray emitting material varies.

6. Conclusions

We have made some of the longest pointed *ROSAT PSPC* observations of early-type stars with the roughly 15 ks observations of four β Cephei variables. These very high signal-to-noise *PSPC* spectra are otherwise typical of late-O and early-B stars. All four of the stars have $L_{\rm X}/L_{\rm Bol} \approx 10^{-7}$ and soft spectral energy distributions. One of the stars, β Cru, has a count rate that is among the highest detected for any hot star.

All four stars show X-ray variability at some level, although only two of them, β Cru and ξ^1 CMa, have detections above the 3 σ level. These are among the strongest detections of X-ray variability in any hot star. Furthermore, the X-ray variability of the program stars is clearly modulated on the same periods as is the optical variability. However, the presence of other frequency components and the relationship between the X-ray and optical phases cannot be determined at this point. In any case, these data represent the first detection of a correlation between activity in the wind of a hot star and its photosphere.

For β Cru, the variability is due to changes principally in the hard X-rays, above 0.5 keV, whereas for the other three stars the variability is dominated by the soft band. This implies that for β Cru, the variation must be in the X-ray *production*, whereas for the other stars, changing wind absorption of X-rays may play an important role in the variability. To the extent that the modulation of the X-rays seen in ξ^1 CMa is due to changes in X-ray production, however, the observed amplitude is large enough that if we are to understand it solely in terms of variations in the available wind material, then the X-ray emission must begin only a few tenths of a stellar radius into the wind flow.

We would like to thank Stan Owocki for several helpful discussions. This research was supported in part by NASA grants NAG 5-2492, NAG 5-3530, and NAG 5-2705.

REFERENCES

Abbott, D. C. 1982, ApJ, 259, 282

Aerts, C., de Cat, P., Cuypers, J., Becker, S. R., Mathias, P., de Mey, K., Gillet, D., & Waelkens, C. 1998, A&A, 329, 137

Aerts, C., Mathias, P., Gillet, D., & Waelkens, C. 1994, A&A, 286, 109

Agrawal, P. C., Singh, K. P., Riegler, G. R., & Stern, R. A. 1984, MNRAS, 208, 845

Beeckmans, F., & Burger, M. 1977, A&A, 61, 815

Berghöfer, T. W., Baade, D., Schmitt, J. H. M. M., Kudritzki, R.-P., Puls, J., Hillier, D. J., Pauldrach, A. W. A. 1996, A&A, 306, 899

Berghöfer, T. W., & Schmitt, J. H. M. M. 1994a, A&A, 292, L5

Berghöfer, T. W., & Schmitt, J. H. M. M. 1994b, Science, 265, 1689

Berghöfer, T. W., & Schmitt, J. H. M. M. 1995, Adv. Space Res., 16, 163

Briel, U. G., et al. 1996, *ROSAT* User's Handbook, Max-Planck-Institut für Extraterrestrische Physik, 85740 Garching, Germany

Cassinelli, J. P., et al. 1996, ApJ, 460, 949

Cassinelli, J. P., Cohen, D. H., MacFarlane, J. J., Sanders, W. T., & Welsh, B. Y. 1994, ApJ, 421, 705

Castor, J. I., Abbott, D. C., & Klein, R. I. 1975, ApJ, 195, 157

Cohen, D. H., Cassinelli, J. P., & MacFarlane, J. J. 1997a, ApJ, 487, 867

Cohen, D. H., Cassinelli, J. P., & Waldron, W. L. 1997b, ApJ, 488, 397

Cohen, D. H., Cooper, R. G., MacFarlane, J. J., Owocki, S. P., Cassinelli, J. P., & Wang, P. 1996, ApJ, 460, 506

Collura, A., Sciortino, S., Serio, S., Vaiana, G. S., Harnden, F. R., & Rosner, R. 1989, ApJ, 338, 296

Cooper, R. G., & Owocki, S. P. 1994, Ap&SS, 221, 427

Corcoran, M. F., et al. 1993, ApJ, 412, 792

Corcoran, M. F., Ishibashi, K., Davidson, K., Swank, J. H., Petre, R., & Schmitt, J. H. M. M. 1997, Nature, 390, 587

Cox, A. N., & Tabor, J. E. 1976, ApJS, 31, 271

Cranmer, S. R. & Owocki, S. P. 1996, ApJ, 462, 469

Drew, J. E., Denby, M., & Hoare, M. G. 1994, MNRAS, 266, 917

ESA 1997, *The Hipparcos and Tycho Catalogues*, ESA SP-1200

Feldmeier, A. 1995, A&A, 299, 523

Feldmeier, A., Puls, J., & Pauldrach, A. 1997, A&A, 322, 878

Frost, E. B. 1902, ApJ, 15, 340

Henrichs, H. F., et al. 1999, in *The Be Phenomenon in Early-Type Stars*, A.S.P. Conference Series, (San Francisco: Astronomical Society of the Pacific), in press

Henrichs, H. F. 1993, in *New Perspectives on Stellar Pulsation and Pulsating Variable Stars*, I.A.U. Colloquium 139, (Cambridge: Cambridge University), 186

Heynderickx, D. 1992, A&AS, 96, 207

Heynderickx, D., Waelkens, C., & Smeyers, P. 1994, A&AS, 105, 447

Hiltner, W. A., Garrison, R. F., Schild, R. E. 1969, ApJ, 157, 313

Iglesias, C. A., & Rogers, R. J. 1991, ApJ, 371, 408

Kaper, L., et al. 1997, A&A, 327, 281

Kiriakidis, M., El Eid, M. F., & Glatzel, W. 1992, MNRAS, 255, 1

Lesh, J. R. 1968, ApJS, 17, 371

Lucy, L. B. & Solomon, P. M. 1970, ApJ, 159, 879

MacFarlane, J. J., & Cassinelli, J. P. 1989, ApJ, 347, 1090

MacFarlane, J. J., Waldron, W. L., Corcoran, M. F., Wolff, M. J., Wang, P., & Cassinelli, J. P. 1993, ApJ, 419, 813

Massa, D., et al. 1995, ApJ, 452, L53

Meurs, E. J. A., et al. 1992, A&A, 265, L41

Moskalik, P., & Dziembowski, W. 1992, A&A, 256, L5

Mullan, D. J. 1984, ApJ, 283, 303

Nordsieck, K. H., Cassinelli, J. P., & Anderson, C. M. 1981, ApJ, 248, 678

Nousek, J.A., & Lesser, A. 1993, *ROSAT* Newsletter, volume 8

Owocki, S. P., Castor, J. I., & Rybicki, G. B. 1988, ApJ, 335, 914

Owocki, S. P. & Cohen, D. H. 1999, ApJ, 520, 833

Pallavicini, R., Golub, L, Rosner, R., Vaiana, G. S., Ayres, T., & Linsky, J. L. 1981, ApJ, 248, 279

Pauldrach, A. W. A., & Puls, J. 1990, A&A, 237, 409

Pfeffermann, E., et al. 1986, Proc. SPIE, 733, 519

Sahade, J., & Struve, O. 1956, PASP, 68, 451

Smith, M. A., Grady, C. A., Peters, G. J., & Feigelson, E. D. 1993, ApJ, 409, L49

Smith, M. A., Robinson, R. D., & Corbet, R. H. D. 1998, ApJ, 503, 877

Sterken, C., & Jerzykiewicz, M. 1993, Space Sci. Rev., 62, 95

Straizys, V., & Kuriliene, G. 1981, Ap&SS, 80, 353

Telting, J. H., Aerts, C., & Mathias, P. 1997, A&A, 322, 493

Trümper, J. 1983, Adv. Space Res., 2, 241

Weiss, A., Keady, J. J., & Magee, N. H. 1990, Atomic Data Nucl. Data, 45, 209

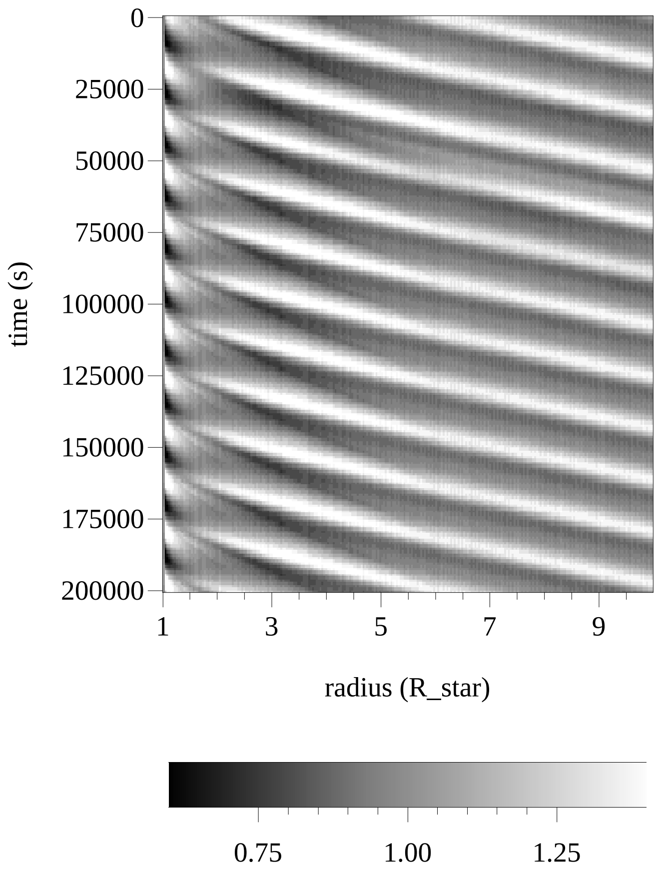

Fig. 3.— Contours of n^2 (cm^{-6}) for a wind driven by a radiation field with a luminosity varying sinusoidally on a 5 hour period. The density is scaled to the density from a steady-state wind and is shown vs. time on the y-axis and vs. radius on the x-axis. The emission measure at any time is given by integrating this quantity along a horizontal line in the figure ($EM = \int_{R_{\rm min}}^{\infty} n^2 4\pi r^2 dr$). It can be seen that several density enhancements will be included in such an integration.